

Photodissociation of HCHO in air: CO and H₂ quantum yields at 220 and 300 K

Cite as: J. Chem. Phys. **78**, 1185 (1983); <https://doi.org/10.1063/1.444911>

Submitted: 25 May 1982 • Accepted: 20 September 1982 • Published Online: 31 August 1998

Geert K. Moortgat, Wolfgang Seiler and Peter Warneck



View Online



Export Citation

ARTICLES YOU MAY BE INTERESTED IN

[CO and H₂ quantum yields in the photodecomposition of formaldehyde in air](#)

The Journal of Chemical Physics **70**, 3639 (1979); <https://doi.org/10.1063/1.437956>

[T₁ barrier height, S₁-T₁ intersystem crossing rate, and S₀ radical dissociation threshold for H₂CO, D₂CO, and HDCO](#)

The Journal of Chemical Physics **87**, 3855 (1987); <https://doi.org/10.1063/1.452940>

[The energy dependence of CO\(v,J\) produced from H₂CO via the transition state, roaming, and triple fragmentation channels](#)

The Journal of Chemical Physics **147**, 013935 (2017); <https://doi.org/10.1063/1.4983138>



Chemical Physics Reviews

First Articles Now Online!

READ NOW >>>

Photodissociation of HCHO in air: CO and H₂ quantum yields at 220 and 300 K

Geert K. Moortgat, Wolfgang Seiler, and Peter Warneck

Max Planck Institut für Chemie (Otto Hahn Institut), D 6500 Mainz, Federal Republic of Germany
(Received 25 May 1982; accepted 20 September 1982)

New data are presented for the quantum yields of CO and H₂ produced in the photodecomposition of formaldehyde. The data were obtained at the two temperatures 220 and 300 K, as a function of wavelength in the spectral range 253–353 nm, and as a function of pressure at the wavelengths 339.3 and 353.1 nm. The influence of temperature occurs mainly on the quenching constants describing the pressure dependence. The results are compared with previous data and improved quantum yield curves are presented for applications in atmospheric chemistry.

INTRODUCTION

In a previous paper¹ concerned with the photodecomposition of formaldehyde, we reported quantum yields for the products CO and H₂ and their dependencies on wavelengths, for experimental conditions resembling those in the atmosphere. The need for simulation arose because of the significance of formaldehyde photolysis to atmospheric chemistry. The latter subject has been discussed in several recent publications,^{2–5} and the various arguments will not be repeated here. One purpose of our study was to determine the relevance to the atmosphere of other laboratory data obtained at reduced pressures and with high concentrations of formaldehyde, conditions contrasting with those in the natural environment. We found that in the 290–330 nm wavelength region the pressure effect is negligible so that the low pressure data are applicable to the atmosphere, whereas at wavelengths greater than 330 nm, collisional quenching of photo-excited formaldehyde is important whereby all quantum yields are reduced to values much less than unity.

Our previous measurements¹ were restricted to temperatures in the vicinity of 300 K, however. Since with increasing height in the atmosphere the temperature decreases to about 200 K in the lower stratosphere before it rises again, we considered it necessary to extend our earlier study, applying lower temperatures in order to explore conceivable effects upon the product quantum yields. One set of measurements was performed at the temperature of 220 K, another set at 300 K to provide comparison. The results are reported below.

It will be useful to recall that formaldehyde admits two photolytic pathways



In air at pressures near 1 atm, the radicals arising from channel (1) react rapidly with oxygen forming two HO₂ radicals and CO. If the concentrations of formaldehyde are kept low, it will escape secondary attack by radicals and the quantum yield for CO is equivalent to the primary quantum yield for formaldehyde loss. The ratio of stable products $R = (\text{H}_2)/(\text{CO})$ then pro-

vides a measure of the extent to which the photolysis channel (2) participates

$$\phi_2 = \phi(\text{CO}) \cdot R,$$

whereas the quantum yield ϕ_1 for process (1) is given by the difference

$$\phi_1 = \phi(\text{CO}) - \phi_2.$$

The premises for using these equations have been discussed in our previous paper.¹ More recent developments concerning the photo-oxidation mechanism of formaldehyde under atmospheric conditions will be discussed later. There are no additional sources of CO or H₂ which would require modification of the expressions for ϕ_1 and ϕ_2 .

EXPERIMENTAL TECHNIQUES

Photolyses were carried out under optically thin conditions using mixtures of about 100 ppmv HCHO in synthetic air filled into cylindrical quartz cells with an internal diameter of 2.0 cm and an internal length of $L = 10.0$ cm. The cells were jacketed to enable cooling with a thermostatted fluid, and they were provided with double windows on each end to prevent frosting. The light flux I_0 emerging from an $f/2$ monochromator (Jobin-Yvon) and entering the photolysis cell was measured with a calibrated thermopile located behind the cell. Window reflectances were measured and appropriate corrections applied. CO quantum yields were calculated from the equation

$$\phi(\text{CO}) = \frac{M(\text{CO}) \cdot n(M) \cdot V}{I_0 \cdot \sigma_{\text{eff}} \cdot n(\text{HCHO}) \cdot A \cdot L \cdot \Delta t}$$

and a corresponding expression was used to determine H₂ quantum yields. The quantities to be measured are: $m(\text{CO})$, the mixing ratio of CO produced in the cell by photolysis; $n(M)$, the total number density of molecules present in the cell, essentially that of air; $n(\text{HCHO})$ and σ_{eff} , the number density and effective cross section of formaldehyde, respectively; V , the volume of the cell; Δt the duration of photolysis; A , the cross section of the light beam, and L and I_0 which were defined above.

The preparation of gas samples, the light source, and the analytical procedures were the same as described previously.¹ A more powerful monochromator

was now used, set to a bandwidth of 5 nm. As previously, two identical cells were used in parallel; one served as the photolysis cell proper, the other was kept in the dark and provided a blank value in the subsequent analysis. Effective absorption cross sections of formaldehyde were remeasured at the wavelengths at which HCHO was photolyzed, using a double beam spectrophotometer with slit settings providing the same spectral resolution as that used in the photolysis runs. Again, a thermostatted absorption cell of the type described above was employed.

For most runs at 220 and 300 K, the total pressure of the gas mixtures was varied between 800 and 200 Torr. An extensive pressure dependence study was done at 353 nm for both temperatures, and somewhat less extensive at 339 nm.

All the experimental conditions and new results on the CO and H₂ quantum yield data have been fully reported earlier⁶ and will not be repeated here.

RESULTS AND DISCUSSION

The coarse spectral resolution provided an HCHO absorption spectrum consisting of ten broad bands. Photolysis runs were done at wavelengths near the band maximum. The effective absorption cross sections were found to depend on concentration, decreasing with increasing formaldehyde content at a number of wavelengths. The admixture of 500–600 Torr of nitrogen reduced the concentration dependence to some extent but did by no means eliminate it. The variation of the effective absorption cross sections with pressure of the absorber for spectra with band structure is a well-known effect resulting from inadequate spectral resolution. Since the center of the rotational lines cause the incident radiation to be attenuated most strongly, a filtering effect ensues, whereby the effective (overall) cross section is gradually lowered. A recent investigation of this effect by a fluorescence technique was performed by Fairchild *et al.*⁷ Formaldehyde partial pressures used in the photolysis experiments are much lower than those employed in measuring absorption

TABLE I. Effective absorption cross sections of HCHO for two temperatures at wavelengths used in the photolysis runs. Spectral resolution 5 nm (previous 3.5 nm).

Wavelength λ (nm)	Effective cross section (10^{-20} cm ²)		
	220 K	298 K	353 K (previous)
353.1	1.11	0.96	0.94
339.3	2.30	2.40	1.81
327.0	3.37	3.60	2.44
315.0	4.60	4.52	3.22
304.1	4.24	4.44	3.58
294.9	3.64	3.48	3.00
285.6	2.90	2.46	2.33
278.1	1.97	1.60	1.55
270.6	1.14	1.00	...
262.0	0.66	0.62	...
253.0	0.30	0.27	...

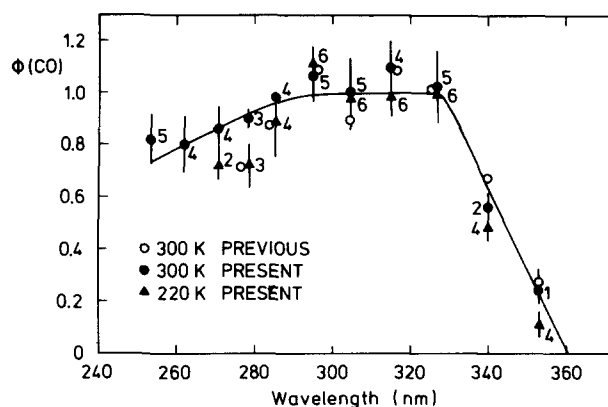


FIG. 1. CO quantum yield from HCHO photolysis as a function of wavelength. \bullet present data at 300 K, \blacktriangle present data at 220 K, \circ data obtained previously (Ref. 1). All data were obtained at pressure near 1 atm. The numbers of runs used for averaging are indicated next to each point.

cross sections (0.076 Torr vs 5–20 Torr). It was thus necessary to take the concentration dependence into account and extrapolate absorption cross sections measured at different concentrations of formaldehyde toward zero concentrations. The extrapolation procedure gave essentially identical cross sections with and without nitrogen addition. Table I lists cross sections obtained in this manner for two temperatures, 298 and 220 K. It can be seen that at all the wavelengths employed the cross sections are practically the same within the error caused by the extrapolation, so that under these conditions the temperature effect is negligible. Our previous photolysis data¹ relied on cross sections measured at 353 K. This temperature was chosen to eliminate a possible polymerization of formaldehyde on the walls of the absorption cell. The procedure becomes questionable, if the effective cross section were strongly temperature dependent. The present results allay such fears. They are nevertheless somewhat higher compared with the cross sections given previously, because the latter were not extrapolated to zero concentrations. We have also obtained HCHO absorption cross sections at the higher spectral resolution of 0.5 nm and have found a more pronounced temperature dependence for some bands (7 bands out of 31). The data have been discussed elsewhere.⁶

Quantum yields for CO and H₂ derived from individual runs were averaged and the results, plotted vs wavelength, are shown in Figs. 1 and 2, respectively, together with our previous data.^{1,8} Figure 3 is added to present, also as a function of wavelength, the ratio of the two quantum yields. In principle, the ratio should be more accurate as it depends only on the calibration of the analytical scheme and does not involve parameters such as the absorption cross section and absolute radiation intensity, which are harder to determine and carry more error. Compared with our previous results,¹ the H₂/CO ratios are slightly higher. The effect is most noticeable in the wavelength region 340–355 nm, where a ratio of unity is expected because the decomposition of formaldehyde into H₂ and CO (channel 2) is

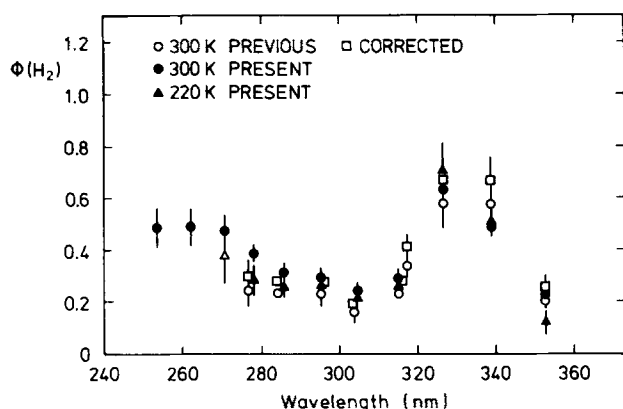


FIG. 2. H_2 quantum yield from HCHO photolysis as a function of wavelength. \bullet present data at 300 K, \blacktriangle present data at 220 K, \circ previous data at 300 K, uncorrected (Ref. 1) \square same data corrected (see the text).

the only energetically allowed process. The present data approach the expected ratio of unity whereas the previous data do not. This problem had been discussed and calibration errors were considered the most likely cause. Although the procedures used now were basically the same as previously,¹ careful attention has been applied to the calibration routine. It appears that conceivable systematic errors have now been minimized.

In our previous discussion of the reaction mechanism of formaldehyde photolysis,^{1,8} we have shown that a great number of conceivable side reactions leading to additional CO and H_2 by processes other than (1) and (2) can be neglected under our experimental conditions. The fate of and possible interference of formic acid, HCOOH, and H_2O_2 have not been considered. It is necessary to assess their importance. Both are produced by reactions of HO_2 radicals resulting from the primary radical products H and HCO. H_2O_2 plus O_2 are formed by the recombination of HO_2 radicals. Formic acid is formed in a complex mechanism following the consecutive addition of the HO_2 radicals to HCHO, via decomposition of the transient HO_2CH_2OH (hydroperoxyhydroxymethane), which was detected by FTIR by Su *et al.*^{9,10} and Niki *et al.*^{11,9} In the chlorine photosensitized HCHO photo-oxidation experiments of Su *et al.*,¹⁰ the rate of CO formation was independent of formaldehyde concentration, unlike the rate of HCOOH formation which increased strongly with increasing formaldehyde concentration (their Fig. 5). Equivalent results were obtained by Su *et al.*¹⁰ in direct photodecomposition experiments of formaldehyde in air, at mixing ratios similar to ours. We conclude, that formic acid does not present a secondary source of carbon monoxide. It adds to the consumption of formaldehyde, however. Using relative rates for CO and HCOOH formation given by Su *et al.*¹⁰ for mixing ratios of 100 ppm HCHO in air, we estimate the amount of HCOOH formation in our system as 1/3 of the rate of CO formation. Maximally, photoconversion yields of formaldehyde to CO in our study were typically 3%. The corresponding losses of formalde-

TABLE II. Rates of CO and OH formation at wavelengths used in the HCHO photolysis (see the text).

Wavelength λ (nm)	CO/ Δt (molecule/s)	OH/ Δt (molecule/s)
270.6	6.0×10^{10}	4.4×10^5
278.1	1.5×10^{11}	3.8×10^6
285.6	3.3×10^{11}	1.1×10^7
294.9	6.6×10^{11}	1.4×10^7
304.4	1.0×10^{12}	2.9×10^7
315.3	6.3×10^{11}	1.8×10^7
327.0	4.4×10^{11}	4.1×10^6

hyde due to conversion to formic acid are 1% at the most. The total consumption of HCHO is still small enough to keep the HCHO number density essentially constant, so that corrections to the measured CO and H_2 quantum yields following from HCHO losses are unnecessary.

As previously we assume that H_2O_2 , like HCOOH, accumulates in the photolysis cell without any further reactions.⁵ Unlike HCOOH,¹² however, hydroperoxide may be subject to photolysis^{13,14} and produce OH radicals¹⁵⁻¹⁷ whose major fate in our system is reaction with formaldehyde. This latter process would be a source of CO. We can estimate the maximum yield of CO by this process assuming that all HO_2 radicals resulting from process (1) to recombine to H_2O_2 . Taking known absorption cross sections for H_2O_2 ,¹⁸ and our experimental parameters, light fluxes, etc.,⁶ we compute the rate of OH formation given in Table II, according to the expression

$$\frac{(OH)}{\Delta t} = 4 \cdot \phi_1 \cdot \phi_2 \cdot \sigma_1 \cdot \sigma_2 \cdot I_0^2 \cdot V^2 \cdot n(HCHO)$$

to be on the average 10^5 times smaller than the rate of CO molecules generated in our system. In the above expression ϕ_1 and σ_1 , and ϕ_2 and σ_2 are the quantum yields and absorption cross sections for HCHO and H_2O_2 , respectively, I_0 is the light flux, V the cell volume, and $n(HCHO)$ the initial HCHO concentration.

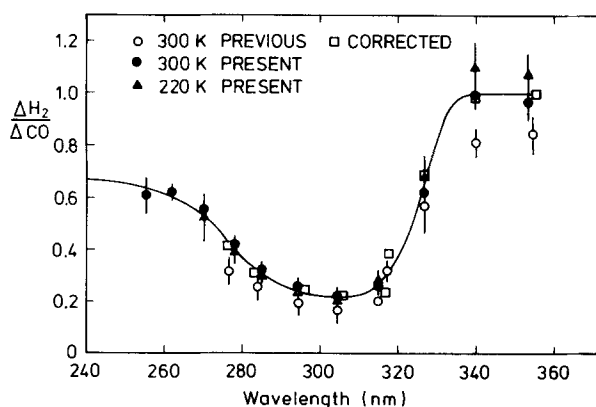


FIG. 3. Ratio of the quantum yield H_2/CO as a function of wave wavelength. \bullet present data at 300 K, \blacktriangle present data at 220 K, \circ previous data at 300 K, uncorrected (Ref. 1), \square same data corrected (see the text).

Even with the accepted rate constant¹⁸ for the reaction $\text{OH} + \text{CH}_2\text{O} \rightarrow \text{CHO} + \text{H}_2\text{O}$ of $1.2 \times 10^{-11} \text{ cm}^3 \text{ molecule}^{-1} \text{ s}^{-1}$, the interference from CO generation via H_2O_2 photolysis is maximal by 0.1% of the total CO yield.

We cannot preclude the possibility that hot H atoms are formed by the photodissociation of HCHO below 300 nm, and of HO_2 below 270 nm, because of its strong absorption features at wavelengths less than 270 nm.^{19,20} Hot H atoms are likely to abstract H atoms from HCHO more efficiently than thermal H atoms and their three-body recombination reactions are slowed down.²¹ In view of the high pressure used in the present experiment, we feel that the hot H atoms would be rapidly thermalized so that this effect is unimportant. Tang, Fairchild, and Lee²² came to similar conclusions.

Table III summarizes the final results of all our measurements^{1,6,8} at 300 K as well as at 220 K. At wavelengths below 330 nm there is no pressure effect and for both temperatures we used data from all runs to compute the averages shown in Figs. 1–3. At longer wavelengths, where pressure quenching occurs, only data obtained with pressures near 1 atm were used. In the spectral region 280–330 nm, the CO quantum yield is unity on average, and no systematic variation with temperature is observed. The decline of CO quantum yields in the 280–290 nm region observed previously in a few runs have not been substantiated, but below 280 nm also the present results indicate a decline. Measurements in this spectral region are made difficult due to unfavorably low light intensities and absorption cross sections which require much

TABLE III. Averages of H_2/CO ratios R (corrected), and H_2 and CO quantum yields as a function of wavelength ($\pm 0.6 \text{ nm}$).

λ (nm)	N	R	ϕ_{H_2}	ϕ_{CO}
(A) 300 K				
253.0	5	0.613 ± 0.073	0.483 ± 0.071	0.818 ± 0.095
262.0	4	0.619 ± 0.029	0.495 ± 0.061	0.801 ± 0.106
270.6	4	0.553 ± 0.025	0.477 ± 0.062	0.862 ± 0.084
277.4	5	0.422 ± 0.058	0.350 ± 0.067	0.828 ± 0.112
284.9	5	0.310 ± 0.016	0.308 ± 0.021	0.965 ± 0.052
295.0	8	0.264 ± 0.022	0.287 ± 0.043	1.082 ± 0.081
304.2	8	0.222 ± 0.024	0.216 ± 0.036	0.964 ± 0.098
315.8	5	0.261 ± 0.016	0.290 ± 0.030	1.114 ± 0.087
371.0	7	0.389 ± 0.042	0.414 ± 0.058	1.090 ± 0.132
326.8	10	0.652 ± 0.094	0.660 ± 0.109	1.021 ± 0.157
339.8	66	0.986 ± 0.026	0.639 ± 0.154	0.645 ± 0.142
354.0	19	0.983 ± 0.096	$0.252 \pm 0.044^{\text{a7}}$	$0.258 \pm 0.040^{\text{a7}}$
(B) 220 K				
270.6	2	0.523 ± 0.090	0.388 ± 0.111	0.717 ± 0.057
278.1	3	0.396 ± 0.052	0.283 ± 0.059	0.728 ± 0.081
285.6	4	0.229 ± 0.022	0.266 ± 0.033	0.894 ± 0.125
294.9	6	0.245 ± 0.017	0.272 ± 0.030	1.111 ± 0.090
304.4	6	0.213 ± 0.016	0.213 ± 0.027	0.998 ± 0.134
315.3	6	0.282 ± 0.027	0.277 ± 0.020	0.986 ± 0.073
327.0	7	0.694 ± 0.057	0.717 ± 0.010	1.030 ± 0.089
339.3	8	1.110 ± 0.085	$0.509 \pm 0.036^{\text{a4}}$	$0.508 \pm 0.095^{\text{a4}}$
353.1	11	1.070 ± 0.073	$0.124 \pm 0.038^{\text{a5}}$	$0.117 \pm 0.032^{\text{a5}}$

a = average of N runs, only at atmospheric pressure.

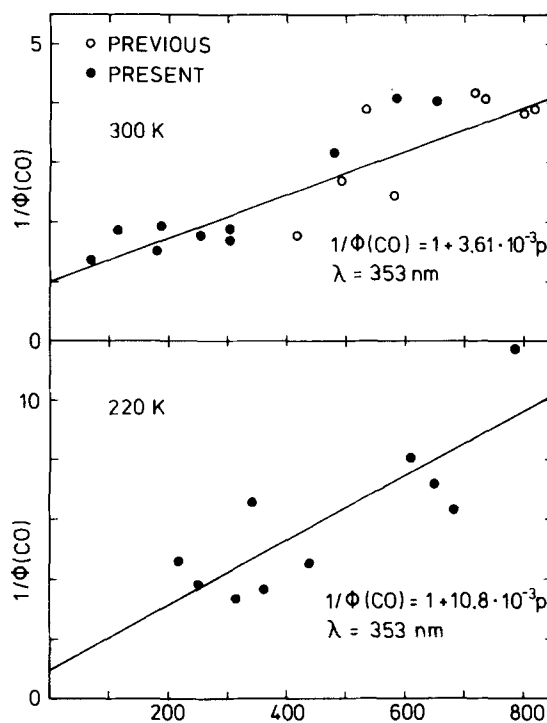


FIG. 4. Stern-Volmer plot of inverse CO quantum yields vs pressure at 300 and 220 K. ● Present data at 353 nm, ○ previous data at 355 nm.

longer photolysis times. It appears that the CO quantum yields decrease toward $\phi(\text{CO}) \approx 0.8$ at 250 nm at room temperature, but since we have found no evidence for a pressure effect we are inclined to attribute the observations of CO quantum yields below unity to measurement difficulties. At 220 K the decline may be even stronger, but the experimental difficulties prevent a cleancut decision about the significance of this effect. Additional studies are required to eliminate these uncertainties.

The pressure dependence of quantum yields in the region above 330 nm was investigated at 353 nm wavelength for both temperatures, 220 and 300 K, and at 339 nm wavelength for 220 K. The variations of CO quantum yields observed at 353 nm are shown in Fig. 4 in the form of a Stern-Volmer plot. The data for 300 K are in good agreement with our previous results and both were used in the least square fit to derive the Stern-Volmer line. The slope of the line gives for the quenching constant the value $\alpha = (3.61 \pm 0.55) \times 10^{-3} \text{ Torr}^{-1}$. It is in good accord with that obtained previously $\alpha = 3.5 \times 10^{-3} \text{ Torr}^{-1}$. The quenching constant found for the lower temperature of 220 K is higher, namely, $\alpha = (10.8 \pm 2.6) \times 10^{-3} \text{ Torr}^{-1}$. Part of the quenching constant is due to the increase of number density when the temperature is lowered while the pressure is kept fixed. This effect can be taken into account by defining the quenching constant in terms of number density rather than pressure. We then obtain the values listed in Table IV. We note that the ratios $\alpha n_{220}/\alpha n_{300}$ are not much different, indicating that the influence of temperature on the quenching constants is essentially the same at both wavelengths.

TABLE IV. Quenching constants α^n for CO quantum yields by air, at 220 and 300 K.

λ (nm)	α^n (10^{-18} cm ³ molecule ⁻¹)		$\alpha^n(220)/\alpha^n(300)$
	220 K	300 K	
353	2.47 ± 0.59	1.12 ± 0.17	2.20 ± 0.86
339	0.39 ± 0.07	0.26 ± 0.10	1.50 ± 0.84

To discuss the influence of temperature on the quenching constant, we note that the quenching constant $\alpha^n = k_q/k_d$ is the ratio of two rate coefficients: that for collisional deactivation k_q , and that for unimolecular dissociation of the excited HCHO molecule k_d . The latter describes an average over dissociation coefficients associated with various energy levels which are populated by photoexcitation and thermal excitation combined. As discussed previously,¹ it is likely that the quenching of CO and H₂ product quantum yields is due mainly to electronic quenching of the S₁ state for which information is available on vibrational and rotational level distribution. In addition, Shibuya and Lee²³ have shown that at least for the 4⁰ and 4¹ vibrational levels, a Boltzmann equilibrium is established on account of collisional deactivation and excitation, and Fairchild *et al.*²⁴ have shown that for rotational levels of the 4⁰ states collisional redistribution of energy also is faster than electronic quenching. If we assume the dissociation rate to increase linearly with the thermal energy content of the HCHO molecule above that due to photoexcitation, we would have

$$k_d = \frac{\sum_i k_{di} \cdot n_i}{\sum_i n_i} = k_0 \left(1 + a \frac{\sum_i n_i E_i}{\sum_i n_i} \right) \\ = k_0 (1 + a \langle E_i \rangle),$$

where k_{di} is the dissociation coefficient and n_i the population of the i th level, respectively. E_i is the asso-

ciated energy, k_0 is the rate coefficient for CO formation from the lowest level, and a is an appropriate constant. We have calculated the average thermal energy content (E_i) for 300 and 220 K, assuming HCHO to be approximated as a symmetric top molecule with respect to rotation, and taking into account only the four lower vibrational levels. The resulting ratio $k_d(300)/k_d(220)$ for favorable values of a (>0.42) is found to lie in the range 1.4–1.5. The result is in reasonable agreement with the experimentally obtained ratios shown in Table IV considering the not appreciable experimental errors. Thus it appears that the influence of temperature on the quenching constants is mainly due to variation in the rate of unimolecular dissociation.

Finally, we discuss the quantum yields for the photodissociation process (1). We have shown previously that for our experimental conditions ϕ_1 is given by the relation

$$\phi_1 = \phi(\text{CO})[1 - \phi(\text{H}_2)/\phi(\text{CO})].$$

To calculate ϕ_1 we make use of the ratios of quantum yields shown in Fig. 3. Appropriate corrections were applied to our previous data to account for calibration errors. The solid line in Fig. 1 was taken to represent the average CO quantum yield. The results are shown in Fig. 5. Also included in this figure are the data of Horowitz and Calvert²⁵ and of Clark *et al.*,²⁶ who measured H₂ quantum yields at reduced pressures in the presence of suitable radical scavengers (C₄H₈ and NO, respectively). All these data are now in very good agreement. It should not go unnoticed that Lee and collaborators have observed H atoms from processes (1) by HNO chemiluminescence.^{22,27,28} We had included quantum yields deduced by these workers in the comparative plot of all ϕ_1 data in a previous paper.¹ All the data of Lewis, Tang, and Lee,²⁷ and of Tang, Fairchild, and Lee²² show appreciable scatter, with most of the data points lying below the solid curve fitting the data in Fig. 5. We have therefore omitted

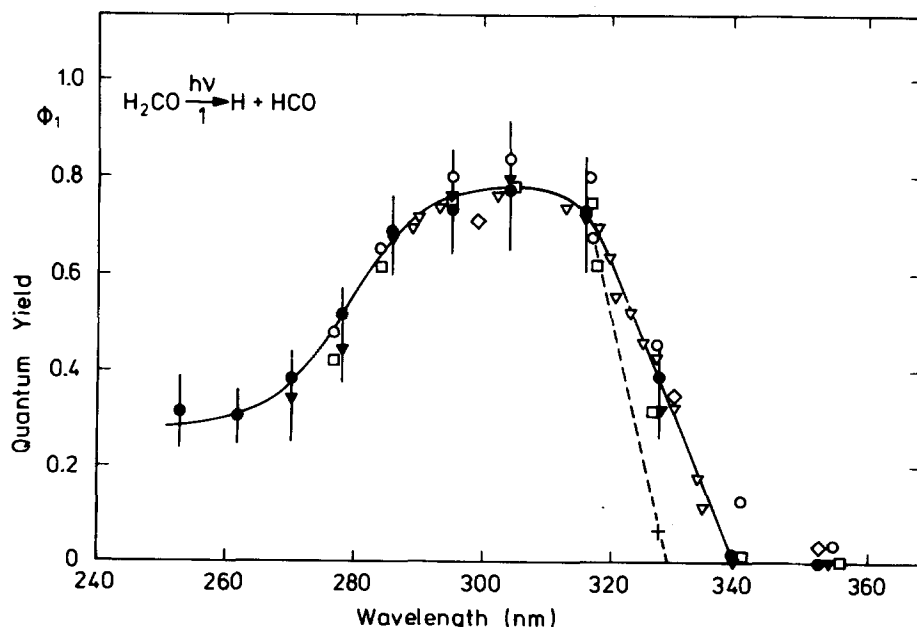


FIG. 5. Quantum yield for radical formation ϕ_1 as a function of wavelength, ● present data at 300 K, △ present data at 220 K, ○ uncorrected previous data (Ref. 1), □ corrected previous data, ▽ data of Horowitz and Calvert (Ref. 25), ◇ data of Clark *et al.* (Ref. 26), + calculated quantum yield at 270 nm for 0 K, --- extrapolation to dissociation threshold wavelength (328.4 nm) at 0 K.

their data in Fig. 5 for the sake of clarity.

At room temperature, the onset of process (1) occurs at 337.9 nm. The corresponding energy is 84.3 kcal/mol. It provides a lower limit to the H-HCO dissociation energy. In this threshold region, however, a certain dependence of ϕ_1 on temperature is expected because the thermal energy contributes to the total energy contained in the formaldehyde molecule after photodissociation. Accordingly, the threshold wavelength of process (1) should be lowered to some extent when the temperature is reduced. Indeed, the data point for 220 K obtained at 327 nm lies markedly below the 300 K data at the same wavelength, whereas the ϕ_1 quantum yields at the three lower wavelengths 316, 304, and 295 nm coincide. If we take this as evidence for the predicted temperature effect and extrapolate ϕ_1 at 327 nm linearly with temperature toward zero degrees, we find the value indicated in Fig. 5 by the cross. The dashed line is entered in Fig. 5 to indicate the predicted behavior of ϕ_1 as a function of wavelength. Specifically, the dashed line extrapolates toward a threshold wavelength of 328.4 ± 2.3 nm, corresponding to an energy of 87.1 ± 0.7 kcal/mol which agrees remarkably well with the measured dissociation energy: 86.9 ± 2 kcal/mol (Walsh and Benson),²⁹ 88.2 ± 1.6 kcal/mol (Warneck),³⁰ 86 ± 1 kcal/mol (Reilly *et al.*),³¹ 84.6 ± 1.5 kcal/mol (Dyke *et al.*),³² and recent theoretical calculations: 89.5 kcal/mol (Hayes),³³ 88.2 kcal/mol (Goddard and Schaefer),³⁴ and 86.1 kcal/mol (Adams *et al.*).³⁵ We thus feel that the deviation of the ϕ_1 value obtained at 220 K from the other data is significant and due to the predicted temperature effect.

ACKNOWLEDGMENTS

This study was supported, in part, by the High Altitude Pollution Program of The U. S. Federal Aviation Administration under Contract DOT-FA78-WA-4264, and by the Deutsche Forschungsgemeinschaft by its Sonderforschungsberich 73, Atmospheric Trace Constituents.

¹G. K. Moortgat and P. Warneck, *J. Chem. Phys.* **70**, 3639 (1979).

²B. J. Finlayson and J. N. Pitts, Jr., *Science* **192**, 111 (1976).

³T. E. Graedel, L. A. Farrow, and T. A. Weber, *Atmos. Environ.* **10**, 1095 (1977).

⁴R. J. Gelinas and P. D. Skewes-Cox, *J. Phys. Chem.* **81**, 2468 (1977).

⁵A. C. Lloyd, *Natl. Bur. Stand. Spec. Publ.* **557**, 27 (1979).

⁶G. K. Moortgat, W. Klippel, K. H. Möbus, W. Seiler, and

P. Warneck, FAA Report no FAA-EE-80-47, Office of Environment and Energy, Washington D.C. 20591, Nov. 1980.

⁷P. W. Fairchild, N. L. Garland, W. E. Howard III, and E. K. C. Lee, *J. Chem. Phys.* **73**, 3046 (1982).

⁸G. K. Moortgat, F. Slemr, W. Seiler, and P. Warneck, *Chem. Phys. Lett.* **54**, 444 (1978).

⁹F. Su, J. G. Calvert, J. H. Shaw, H. Niki, P. D. Maker, C. H. Savage, and J. P. Breitenbach, *Chem. Phys. Lett.* **65**, 221 (1979).

¹⁰F. Su, J. G. Calvert, and J. H. Shaw, *J. Phys. Chem.* **83**, 3185 (1979).

¹¹H. Niki, P. D. Maker, C. M. Savage, and L. P. Breitenbach, *Chem. Phys. Lett.* **75**, 533 (1980).

¹²J. G. Calvert and J. N. Pitts, Jr., *Photochemistry* (Wiley, New York, 1967), p. 428.

¹³L. T. Molina, S. D. Schinke, and M. J. Molina, *Geophys. Res. Lett.* **4**, 580 (1977).

¹⁴C. L. Lin, N. K. Rohatgi, and W. B. DeMore, *Geophys. Res. Lett.* **5**, 113 (1978).

¹⁵D. H. Volman, *Adv. Photochem.* **1**, 69 (1963).

¹⁶L. J. Stief and V. J. De Carlo, *J. Chem. Phys.* **50**, 1234 (1969).

¹⁷N. R. Greiner, *J. Chem. Phys.* **45**, 99 (1966).

¹⁸D. L. Baulch, R. A. Cox, R. F. Hampson, Jr., J. A. Kerr, J. Troe, and R. T. Watson, *J. Phys. Chem. Ref. Data* **9**, 295 (1980).

¹⁹T. T. Paukert and H. S. Johnston, *J. Chem. Phys.* **56**, 2824 (1972).

²⁰C. J. Hochanadel, J. A. Ghormley, and P. J. Ogren, *J. Chem. Phys.* **56**, 4426 (1972).

²¹F. S. Rowland, *Med. Technol. Publ. Co., Int. Rev. Sci.: Phys. Chem.*, Ser. One **9**, 106 (1972). Edited by Polanyi (Butterworths, London, England).

²²K. Y. Tang, P. W. Fairchild, and E. K. C. Lee, *J. Phys. Chem.* **83**, 569 (1979).

²³K. Shibuya and E. K. C. Lee, *J. Chem. Phys.* **69**, 758 (1979).

²⁴P. W. Fairchild, K. Shibuya, and E. K. C. Lee, *J. Chem. Phys.* **75**, 3407 (1981).

²⁵A. Horowitz and J. G. Calvert, *Int. J. Chem. Kinet.* **10**, 805 (1978).

²⁶J. H. Clark, C. B. Moore, and N. S. Nogar, *J. Chem. Phys.* **68**, 2910 (1976).

²⁷R. S. Lewis, K. Y. Tang, and E. K. C. Lee, *J. Chem. Phys.* **65**, 2910 (1976).

²⁸R. S. Lewis and E. K. C. Lee, *J. Phys. Chem.* **82**, 249 (1978).

²⁹P. Walsh and S. W. Benson, *J. Am. Chem. Soc.* **88**, 4570 (1966).

³⁰P. Warneck, *Z. Naturforsch. Teil A* **26**, 2047 (1971).

³¹J. P. Reilly, J. H. Clark, C. B. Moore, and G. C. Pimentel, *J. Chem. Phys.* **69**, 4381 (1978).

³²J. M. Dyke, N. B. H. Jonathan, A. Morris, and M. J. Winter, *Mol. Phys.* **39**, 629 (1980).

³³D. M. Hayes and K. Morokuma, *Chem. Phys. Lett.* **12**, 539 (1972).

³⁴J. D. Goddard and H. F. Schaefer III, *J. Chem. Phys.* **70**, 5117 (1979).

³⁵G. T. Adams, G. D. Bent, R. J. Barlett, and G. D. Purvis, *J. Chem. Phys.* **75**, 834 (1981).